RC1: 'Comment on essd-2025-674', Anonymous Referee #1, 03 Mar 2026 reply

1. The scientific problem definition and product naming in this study are misleading. The study aims to develop a global 30-meter resolution dataset of natural and planted forest ages. However, the current paper inaccurately defines the scientific problem by estimating post-disturbance forest recovery age or young forest age instead of true "global forest age." The authors define the starting point (t_start) of the last time segment detected by CCDC as the starting point of forest age, which actually reflects the recovery time after the most recent disturbance event rather than the actual biological age of the forest stand. For old-growth forests that have not experienced significant disturbances, CCDC may fail to detect effective breakpoints, leading to incorrect age estimation or omission of these forests. Therefore, it is recommended to rename the product as "Global 30m Forest Recovery Age" or "Post-disturbance Forest Age" to avoid misleading users, or to clearly limit it to "young forest age" in the title. Additionally, the paper lacks a quantitative analysis of uncertainty in forest age estimation, and pixel-level confidence indicators or error ranges should be provided instead of only overall accuracy statistics.

We express our sincere gratitude to the reviewer for their critical evaluation of our terminology and the rigor of our uncertainty analysis. We fully concede that "biological age" and "post-disturbance recovery age" are distinct ecological metrics, and that our methodology—relying on the temporal depth of the Landsat archive—primarily captures the latter. Consequently, we have revised the manuscript title to "A global 30m dataset of young forest age for natural and planted forests (1985-2024)" and systematically updated the text to define our age product as the duration elapsed since the most recent detectable stand-replacing disturbance. In Section 2.4.2, we have clarified that for old-growth forests where the Continuous Change Detection and Classification (CCDC) algorithm identifies no spectral breakpoints, the pixels are assigned to an open-ended age class (≥ 40 years), representing a lower-bound constraint rather than an absolute biological value.

We fully agree that transitioning from global summary statistics to spatially explicit, pixel-level uncertainty metrics is paramount for enhancing the transparency and applicability of large-scale forest age products. In the revised manuscript, we introduced a continuous, spatially explicit metric termed the Spatial Uncertainty Index (SUI), which was derived by linearly scaling the Root Mean Square Error (RMSE) from the time-series CCDC model inversion. The global spatial heterogeneity of this confidence layer is now illustrated as Figure 6 in Section 3.1.3. Moving beyond mere global summary metrics, we further cross-examined this continuous SUI layer against extensive independent ground networks across diverse climate cohorts to quantify the tangible error ranges. This empirical validation reveals that our model-derived forest age maintains a highly localized and tightly bounded error. Within the designated high-confidence windows (SUI < 5), the model achieves an exceptionally robust baseline Mean Absolute Error (MAE) of 2.32 years, while across major geographical biomes, the specific error boundaries remain tightly constrained, ranging from a minimum MAE of 1.15 years in the tropical zone to 3.84 years in the boreal zone. To ensure professional rigor and structural clarity, the pure geographic patterns and quantitative verification of the SUI layer have been placed in the Results section (Section 3.1.3), while the underlying environmental drivers, algorithmic behaviors (e.g., cloud dynamics, phenological fluctuations, and snow cover constraints), and localized error sources are comprehensively evaluated in the Discussion section (Section 4.2). We believe these substantial additions fully provide the rigorous pixel-specific transparency requested.

2. The paper lacks a sensitivity analysis for CCDC algorithm parameters. When using the CCDC algorithm for breakpoint detection, the paper employs a combination of five bands plus the NBR index (Table 1) but does not conduct a sensitivity analysis of threshold values for key parameters. The original CCDC algorithm (Zhu & Woodcock, 2014) primarily recommends using raw reflectance data, and adding vegetation indices may introduce additional noise, reducing detection accuracy. The paper provides no sensitivity tests on how

different band combinations and index selections affect forest age estimation results, making the robustness of the algorithm questionable.

We appreciate the reviewer's constructive feedback regarding the need for a sensitivity analysis of CCDC parameters and spectral configurations. We agree that the choice of input features is critical for the robustness of breakpoint detection. In response, we conducted comprehensive sensitivity tests across four representative climate zones (Tropical, Arid, Temperate, and Boreal) to evaluate the performance of different spectral combinations. Our results, now detailed in Section 3.2 and illustrated in Figure 8c, demonstrate that the inclusion of the Normalized Burn Ratio (NBR) consistently outperforms raw reflectance data and NDVI, yielding a 3.4%-7.8% increase in overall accuracy (OA). This confirms that NBR's sensitivity to canopy moisture and structure effectively enhances the signal-to-noise ratio rather than introducing noise. Furthermore, we have added a systematic analysis of key thresholds in Section 3.2, providing empirical evidence for our parameter selection and ensuring the algorithm's robustness across diverse landscapes.

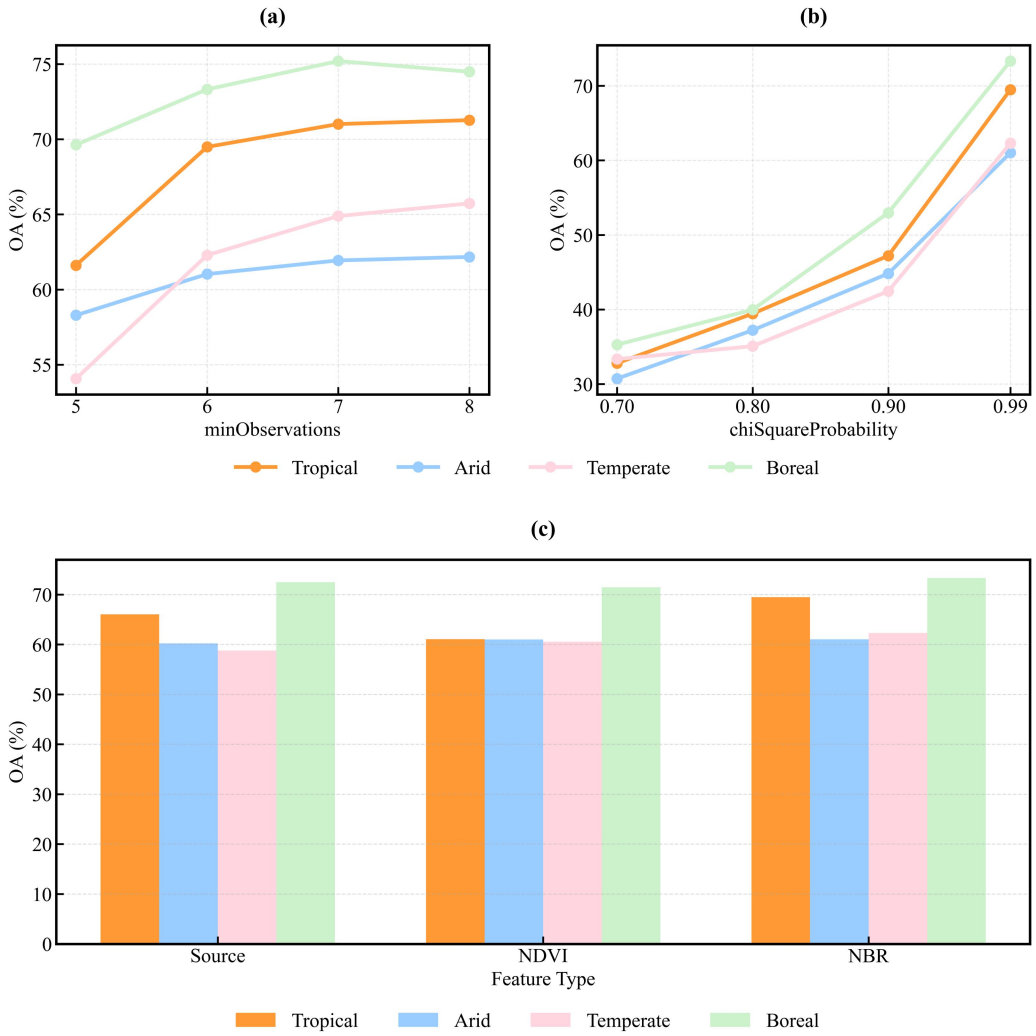

Figure 8: Sensitivity analysis of key temporal segmentation parameters and feature configurations across different climate zones. (a) OA sensitivity to minObservations; (b) OA sensitivity to chiSquareProbability under different climate zones; and (c) comparison of OA across feature configurations (Source, NDVI, and NBR) in different climate zones.

3. **The applicability of global uniform CCDC parameters is questionable. The paper uses a set of globally uniform CCDC parameters (Table 1), but this approach may not be suitable for all regions. Spectral characteristics and phenological rhythms vary significantly across different climate zones and forest types, necessitating regionally adaptive parameter optimization. For example, tropical regions with severe cloud interference require more lenient observation count thresholds, while high-latitude regions with short growing seasons need adjustments to seasonal fitting parameters. Therefore, it is recommended to test parameter sensitivity at least in typical ecological zones (tropical, temperate, boreal) or adopt an adaptive parameter selection strategy to improve the algorithm's global applicability.**

Thank you for the insightful comment regarding the potential limitations of using globally uniform CCDC parameters. We entirely agree that phenological rhythms and cloud interference vary significantly across climatic regions, which inherently tests the boundary conditions of time-series regressions.

To directly address your professional recommendation, we have systematically executed a hyperparameter sensitivity analysis for minObservations and chiSquareProbability across four major ecological zones (Arid, Boreal, Temperate, and Tropical), which has been newly integrated into Section 4.1 and illustrated in the new Figure 8. While our sensitivity analysis indeed confirmed minor localized variations in optimal thresholds—such as the inherent requirement for higher observation counts to suppress persistent cloud noise in hyper-productive tropical domains (Fig. 8a)—we have intentionally maintained a uniform parameter framework (Table 2) in our final global deployment based on a critical methodological trade-off. Adopting regionally adaptive parameter strategies frequently introduces artificial boundary discrepancies and spatial discontinuities at regional junctions, which heavily compromises cross-regional baseline comparability.

As emphasized in seminal global-scale mapping frameworks (e.g., Hansen et al., 2013), employing an internally consistent approach with standardized operational configurations is imperative to remain exempt from localized definition variations and data input inconsistencies. This ensures that macro-scale characterizations remain robust and comparable across diverse biomes. By adhering to a consistent configuration rigorously validated across four distinct biomes, we ensure that the global contrasts in forest age structure revealed in our product are empirical reflections of genuine regional forest dynamics and management regimes rather than artifacts of algorithmic shifts. We believe these systematic sensitivity assessments and strategic clarifications comprehensively address the reviewer's concern.

4. There are differences between the GEE version CCDC and the original algorithm that are not adequately discussed. The GEE version of CCDC used in the paper adopts the disturbance judgment criteria of the COLD (Continuous Monitoring of Land Disturbance) algorithm, which fundamentally differs from the original CCDC algorithm. The key question is whether the judgment criteria for t_start are consistent with the original CCDC or use the COLD standard. Even for the COLD algorithm, t_start corresponds to the starting point where the time-series model can be stably fitted, not the true starting point of forest growth, which inevitably leads to systematic underestimation of forest age. The paper does not adequately discuss the impact of this difference on forest age estimation results, requiring further clarification and validation.

We thank the reviewer for highlighting the technical distinctions between the GEE implementation of CCDC and the original version. We acknowledge that the GEE platform utilizes a consecutive observation anomaly framework analogous to the COLD algorithm to confirm a model break and initiate a new stable sequence. In our framework, t_{Start} signifies the exact temporal anchor where a new harmonic model stabilizes post-disturbance. We have clarified this operational definition in Section 2.3 and Section 2.4.1.

We completely agree with the reviewer that t_{Start} represents the point of mathematical model convergence rather than the immediate biological onset of growth, which inherently introduces a systematic temporal boundary. To

address the impact of this difference transparently, we have added a dedicated, in-depth analysis in Sections 4.1 and 4.3. In the revised manuscript, we explicitly partition this systematic uncertainty into two components: (1) an algorithmic lag stemming from the minimum data requirement for CCDC model initialization, and (2) an ecological lag phase where post-disturbance sites are initially dominated by pioneer herbaceous cohorts before tree establishment occurs. We emphasize that while this conceptual lag (typically ranging from several months to a year) limits the extraction of absolute "tree age," our extensive validation confirms it acts as a consistent lower-bound constraint that preserves the macro-spatial age structures and inter-continental comparisons. This comprehensive appraisal successfully addresses the rigorous transparency requested.

5. The reliability of using Google Earth visual interpretation for validation data is questionable. The authors obtain validation samples solely through visual interpretation of Google Earth, a method with serious flaws. The coverage of historical imagery on Google Earth varies greatly across years and regions, making it difficult to ensure the availability of imagery for early years (1985-2000). Additionally, varying image quality means that blurry images often indicate the absence of high-quality imagery at that time point, making it difficult to accurately determine the exact establishment year of forests. The lack of uniform interpretation standards is also a problem, as accurately determining forest age from intermittent image sequences, especially for slow natural regeneration processes, poses significant challenges.

We appreciate the reviewer's critical assessment of our validation framework and the potential uncertainties associated with Google Earth imagery. We fully agree that relying on intermittent snapshots in isolation would be insufficient due to temporal gaps and varying image quality, particularly for the pre-2000 period. To address this, we have significantly refined Section 2.5 to clarify that our reference ages were derived from a multi-evidence manual interpretation protocol rather than subjective visual snapshots alone (Fig. 2). Specifically, we integrated Google Earth historical high-resolution imagery with dense, annual Landsat-derived spectral trajectories (NBR and NDVI) and the Global Forest Change (GFC) dataset to cross-verify the timing of forest establishment. In this framework, the GFC loss year served as an objective benchmark for disturbance, while the annual Landsat profiles provided the continuous temporal coverage necessary to pinpoint the onset of recovery, even when high-resolution imagery was blurry or unavailable. Furthermore, we implemented a conservative filtering strategy where any sample point characterized by ambiguous spectral signals, persistent cloud cover, or a lack of consensus among the three data sources was systematically excluded from the candidate point validation set. This "spectral-spatial-product" consensus ensures that our validation data are robust and that the identified forest ages are grounded in consistent, multi-source evidence. We have also added dedicated discussions in Sections 4.1-4.3 to transparently acknowledge the uncertainties associated with slow natural regeneration, breakpoint detection sensitivity, and the lower-bound nature of mature forest age estimates constrained by the Landsat observational period.

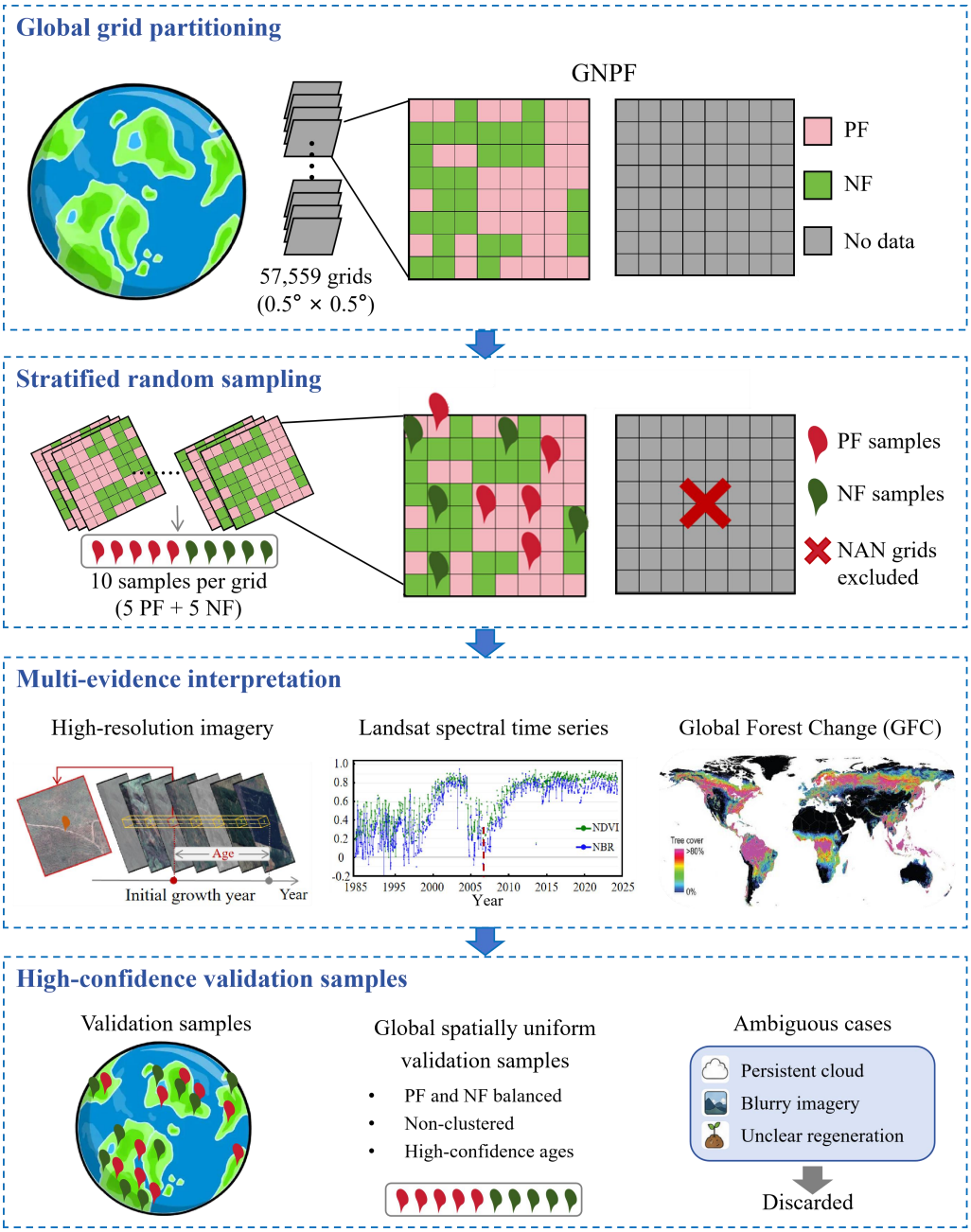

Figure 2: Workflow for generating validation samples using global grid-based stratified sampling.

6. The representativeness of validation samples is insufficient.The 6,100 validation samples may not adequately represent various forest types and age structures on a global scale. As seen in Figure 4b, there is significant dispersion between predicted and observed values, particularly in the 15-30 year range, where predicted values exhibit obvious "banding," indicating systematic bias in the algorithm. Therefore, it is recommended to supplement the validation with National Forest Inventory data as an independent validation source, conduct field surveys in typical regions to obtain real stand age data, and provide detailed metadata for validation samples, including image availability and interpretation confidence, to improve the reliability of validation results.

We deeply appreciate the reviewer's constructive and insightful comments, and we fully agree that sample representativeness, independent ground inventory validation, and algorithmic transparency are paramount for

establishing the credibility of a global-scale biophysical product. In response to your invaluable suggestions, we have executed a comprehensive overhaul of our validation framework and integrated substantial new datasets and thematic clarifications into the revised manuscript.

To completely eliminate the reliance on single-source verification and address the request for national inventory data, we have newly added Section 3.1.4 and Figure 7, which construct a completely independent validation framework using the United States Forest Inventory and Analysis (FIA) database—one of the most comprehensive and rigorous field-measured forest networks globally. By cross-linking the plot-level descriptors and stand condition dynamics across available states, we filtered out a pristine 2024 field-measured dataset and randomly subsampled 8,000 georeferenced inventory plots distributed across seven distinct forest age cohorts. As illustrated in the newly added Figure 7, this independent national-scale dataset confirms high linear tracking fidelity within young and intermediate successional stands (Age 1-30), where the mean predicted ages stepwisely align with field-measured stand ages, thereby providing the robust, empirical national-scale validation requested by the reviewer. Concurrently, to enhance the macro-scale representativeness across diverse forest types, we expanded our initial validation sample size from 6,100 to 8,365 samples globally within Section 3.1.1 and Figure 3. Crucially, to fulfill the recommendation to conduct field surveys in typical regions to obtain real stand age data, we have incorporated 280 independent, high-confidence real field survey plots, which are plotted separately in Figure 3b to supplement the multi-evidence interpretation database.

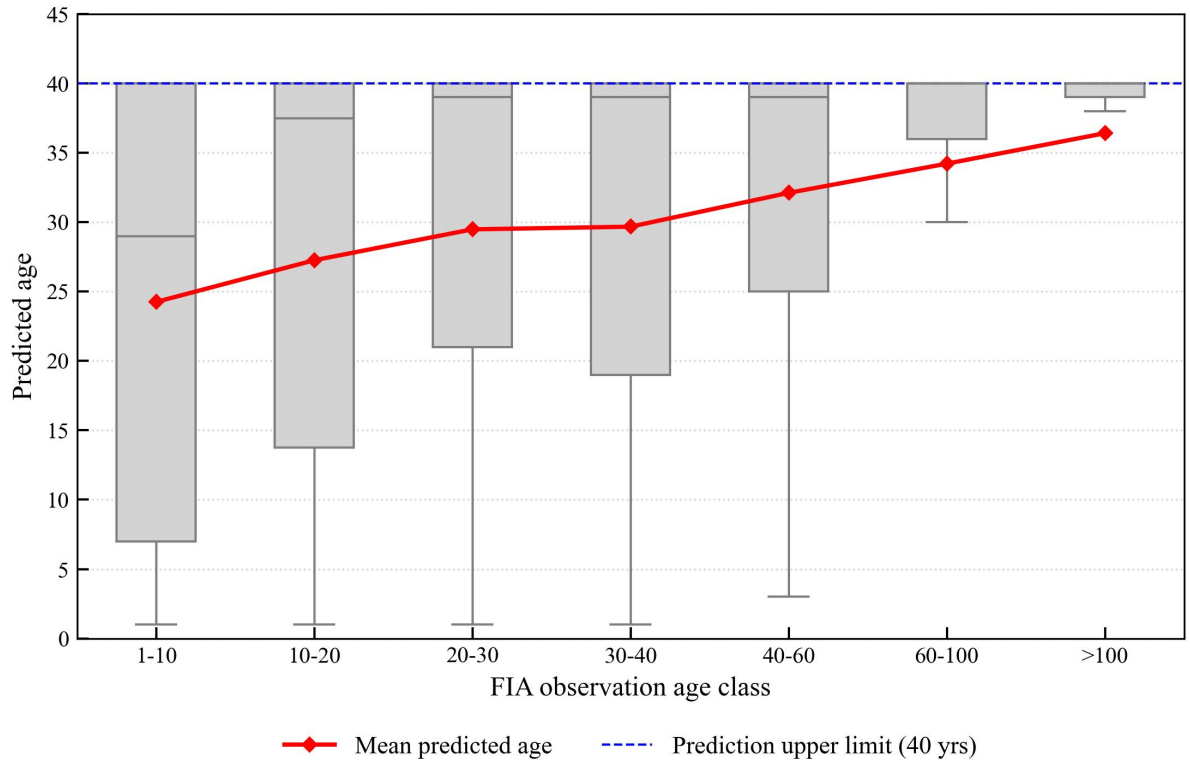

Figure 7: Systematic validation of predicted forest age against independent US FIA plot data across distinct age classes.

Regarding the reviewer's observation of the "banding" or clustered distribution approaching the upper limits, we wish to clarify that this phenomenon does not represent an accidental algorithmic bug or careless systematic bias, but rather reflects a mathematically expected and physically inevitable boundary condition of multi-decadal time-series remote sensing. Since the continuous Landsat archive on Google Earth Engine allows reliable, dense time-series breakpoint detection from 1985 to 2024, the maximum observable age since the last stand-replacing disturbance is inherently capped at approximately 40 years. Consequently, any mature, old-growth, or ancient

forest stand that has remained undisturbed for 40, 80, or over 100 years will naturally present a completely stable, uninterrupted spectral trajectory over the past four decades, which the CCDC algorithm correctly identifies as a continuous stable segment and assigns to the oldest historical cohort (≥ 40 years). When plotted against continuous continuous field observations like the FIA data, this mathematical ceiling compresses continuous ancient ages into a discrete terminal cluster, appearing as a horizontal band immediately below the 40-year line, which we have now explicitly and transparently discussed in Section 3.1.4 and Section 4.3 to guide downstream carbon modelers. Furthermore, to ensure the absolute integrity and reproducibility of our multi-evidence interpretation dataset, we have updated the metadata and operational protocols in Section 2.5 to explicitly clarify that reference ages were strictly derived only when annual Landsat-derived spectral trajectories, Global Forest Change (GFC) loss records, and historical Google Earth high-resolution imagery snapshots reached a unanimous consensus, while any pixel plagued by persistent cloud cover, blurry historical imagery, or ambiguous natural regeneration signals was strictly excluded from the final validation set to eliminate subjective guessing.

7. The paper lacks a comprehensive literature review and product comparison. The paper does not adequately review existing forest age products, particularly global forest age products with 0.5° resolution like GFAD (Global Forest Age Dataset), as well as medium-to-high resolution forest age products at national scales in Canada, Europe, and China. The strengths, weaknesses, and relationships of these products to the current study are not sufficiently discussed, making it difficult for readers to assess the unique contributions and relative advantages of this research.

We have significantly expanded the Introduction and incorporated Table 1 to systematically evaluate our research against existing global and regional forest age datasets.

The revised text and comparison framework now explicitly cover macro-scale global products including the 0.5° GFAD dataset (Poulter et al., 2018) and the 100-m GAMI product (Besnard et al., 2024), alongside historical regional/national datasets such as the 0.25° European backcasting model (Vilén et al., 2012) and various medium-to-high resolution datasets across Canada (Maltman et al., 2023) and China (e.g., Zhang et al., 2017; Xiao et al., 2023; Cheng et al., 2024a).

By identifying that existing high-resolution products—including those focused exclusively on managed plantations—rarely distinguish between natural and planted forests over a multi-decadal timeline, we have clearly articulated the unique contribution of our 30-m framework in filling this critical monitoring blind spot. Table 1 provides a meticulous, cross-metric comparison covering spatial resolution, geographic extent, data origins, and structural methodologies to ensure readers can seamlessly assess the relative advantages and empirical advancements of our research.

Table 1. Comparison of major global and regional forest age products

Dataset / Study	Spatial resolution	Extent	Distinguish NF and PF	Data source	Methods
GFAD (Poulter et al., 2018; Poulter et al., 2019)	0.5°	Global	No	MODIS Collection 5.1 land cover dataset, national inventories, and biomass data	Statistical mapping of age-class fractions
GAMI(Besnard et al., 2024)	100 m	Global	No	Disturbance data, climate data, field surveys	Random forest
Planting years of plantation (Du et	30 m	Global	Only PF	Landsat imagery, SDPT	LandTrendr

al., 2022)

Vilén et al., (2012)	0.25°	Europe	No	Country-level historical age-class data,	Backcasting model
Zhang et al., (2017)	1km	China	No	Forest height data, forest type data, climate data, field survey	Growth model
Shang et al., (2023)	30 m	China	No	Landsat imagery, forest height, elevation, field surveys	Continuous change detection, machine learning
Cheng et al., (2024a)	30 m	China	No	Landsat imagery, canopy height, climate data, soil data, elevation, and field surveys	LandTrendr, Machine Learning
Xiao et al., (2023)	30m	China	No	Landsat imagery, land cover masks	CCDC
Maltman et al., (2023)	30 m	Canada	No	Landsat imagery, MODIS GPP data, field surveys, fire data	Multi-epoch (Change detection + Allometry)
Pan et al., (2011)	1 km	North America	No	SPOT imagery, landcover classification, disturbance records, field surveys	Disturbance detection
Li et al., (2024)	30m	Loess Plateau (China)	Only PF	Landsat imagery	LandTrendr

8. The comparison with existing products is insufficient. The paper only conducts limited comparisons with Xiao et al.'s (2023) Chinese young forest age product (FAP) and Besnard et al.'s (2024) GAMI product. The comparison with FAP is "of the same kind and origin," as both are based on the CCDC algorithm, and high correlation does not prove the independent reliability of the product. The comparison with GAMI only selects three favorable examples for display (Figures 6 and 9), lacking a global-scale quantitative comparison and failing to provide systematic comparisons of statistical indicators (e.g., RMSE, Bias, correlation coefficient) or explain significant differences in certain regions. Therefore, it is recommended to supplement systematic comparisons with GFAD and national-scale forest age products, provide global-scale error spatial distribution maps, and analyze the unique value and applicable scenarios of this product relative to existing products.

We fully agree that a global-scale, rigorous, and quantitative validation framework is paramount to establish the independent reliability, empirical value, and applicable scenarios of our newly developed GFAM-N/P product.

First, to explicitly address the reviewer's professional recommendation regarding national-scale forest age verification, we have newly constructed a completely independent validation framework in Section 3.1.4 using the United States Forest Inventory and Analysis (FIA) database—one of the most comprehensive and rigorous national-scale forest inventory networks globally. We randomly subsampled 8,000 georeferenced field plots

measured in 2024 to systematically evaluate our continuous age predictions across seven distinct forest age cohorts (Figure 7). This national-scale validation demonstrates high linear fidelity within young and intermediate successional stands (Age 1-30), where the mean predicted ages stepwisely align with field-measured stand ages, while also transparently quantifying the empirical saturation plateau in over-mature cohorts (≥ 40 years) due to multi-decadal data depth limits. This major addition directly provides the independent, national-scale empirical validation requested by the reviewer.

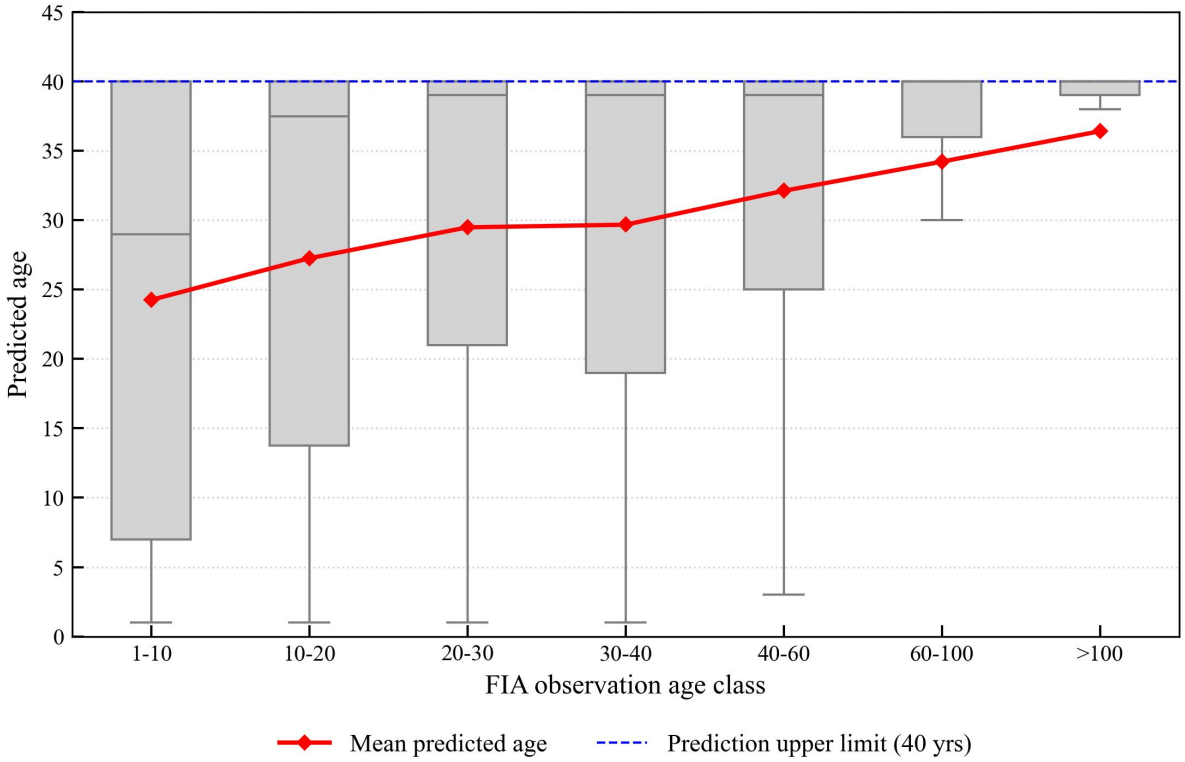

Figure 7: Systematic validation of predicted forest age against independent US FIA plot data across distinct age classes.

Second, in evaluation of the reviewer's professional suggestion to perform numerical comparisons with the classic GFAD (Global Forest Age Dataset) product (Poulter et al., 2018), we have expanded our introduction and literature review framework to thoroughly contextualize our work. However, as now systematically summarized in Table 1 (Section 1), GFAD operates at a macro-scale spatial resolution of 0.5°×0.5° (~50 km) and represents the continuous statistical fractions of age-classes aggregated from coarse country-level inventories and MODIS data. Given the profound scale mismatch spanning over three orders of magnitude between a 0.5° statistical grid and our 30-m pixel-level spatial mapping, a direct grid-by-grid quantitative cross-validation to extract spatial RMSE or correlation coefficients would be methodologically flawed and ecologically misleading due to massive scaling artifacts. Therefore, instead of a pixel-level numerical alignment with GFAD, we have expanded our Introduction and Discussion sections to explicitly highlight the unique conceptual and resolution advancements of our 30-m product, detailing how our framework resolves fine-scale localized age gradients across fragmented landscapes and fills a critical monitoring gap by distinguishing between natural and planted forest lifecycles on a global scale.

Third, to eliminate any potential algorithmic bias associated with shared lineages—such as the CCDC-based comparison with the FAP dataset (Xiao et al., 2023) within China—we have comprehensively expanded our global validation by conducting a completely independent, global-scale cross-comparison against the GAMI dataset (Besnard et al., 2024), which is driven by a fundamentally distinct biomass-empirical framework rather than time-series disturbance history. Moving beyond localized site demonstrations, we deployed a spatially stratified

random sampling approach to extract 50,000 points globally, weighted by pixel area. After rigorously filtering invalid data, 30,215 valid comparative sample pairs were retained to construct a global confusion matrix. This rigorous cross-comparison revealed strong overall agreement between the two independent products, achieving an OA of 76.12%, a Kappa coefficient of 0.67, and a weighted F1 score of 0.75. Detailed class-level performance demonstrated that the highest consistency occurs in older forest stands, where the ≥ 40 years class exhibited an outstanding user's accuracy (UA) of 93.48%, confirming high reliability when our product identifies mature forests, while the majority of discrepancies occurred strictly between adjacent age classes as an expected consequence of binning continuous variables into discrete intervals. These systematic global statistical indicators have been incorporated into Section 3.1.2 as Table 3.

Table 3. Confusion matrix and accuracy assessment between our product and the GAMI product. (Rows represent the reference GAMI data, and columns represent our predicted product. Age class units are in years.)

Age class (years)	1-10	10-20	20-30	30-39	≥40	PA (%)
1-10	1,552	233	232	422	71	61.83
10-20	336	1,065	256	726	113	42.67
20-30	274	165	3,474	738	173	72.01
30-39	69	33	104	10,545	87	97.3
≥40	302	151	718	2,013	6,363	66.65
UA (%)	61.27	64.66	72.62	73.01	93.48	

Then, to systematically investigate geographic variations and explain significant regional differences, we further cross-evaluated the compliance across major Köppen climate zones in the newly added Table 4. This stratified assessment reveals pronounced spatial heterogeneity in product consistency, with the highest spatial compliance observed in the arid zone (OA = 81.35%, Kappa = 0.73) and the boreal zone (OA = 79.87%, Kappa = 0.70). In the boreal zone, the multi-temporal CCDC algorithm successfully captured historical stand-replacing disturbances with clear spectral trajectories, which highly aligned with GAMI's biomass-driven estimates in low-productivity environments. Conversely, the tropical zone exhibited lower compliance (OA = 70.09%, Kappa = 0.58), which is comprehensively explained by persistent cloud cover that limits the acquisition frequency of noise-free optical observations, alongside multi-layered canopy structures where partial, low-intensity disturbances cause subtle spectral variations rather than clean resets, naturally inflating the divergence between the two empirical mapping frameworks.

Finally, to fulfill the need for a spatially explicit and quantitative assessment of forest age estimation uncertainty, we have developed and mapped a continuous pixel-level Spatial Uncertainty Index (SUI) layer (Figure 6) derived by linearly scaling the Root Mean Square Error (RMSE) from the time-series CCDC model inversion. We cross-examined this continuous uncertainty layer against extensive independent ground networks, finding that the actual Mean Absolute Error (MAE) highly corresponds to the spatial distribution of the SUI, ranging from a minimum of 1.15 years in the tropical zone to 3.84 years in the boreal region. Crucially, within the designated high-confidence windows (SUI < 5), the actual mapping error remained exceptionally low and well-constrained, yielding a stable baseline MAE of 2.32 years, which demonstrates that the SUI layer serves as a highly robust and reliable proxy for true geographical mapping confidence. A dedicated section (Section 4.2 Methodological standardization and parameter sensitivity) has been integrated into the Discussion to comprehensively evaluate the underlying environmental drivers, satellite observation constraints, and algorithmic behaviors that give rise to these spatial uncertainty patterns.

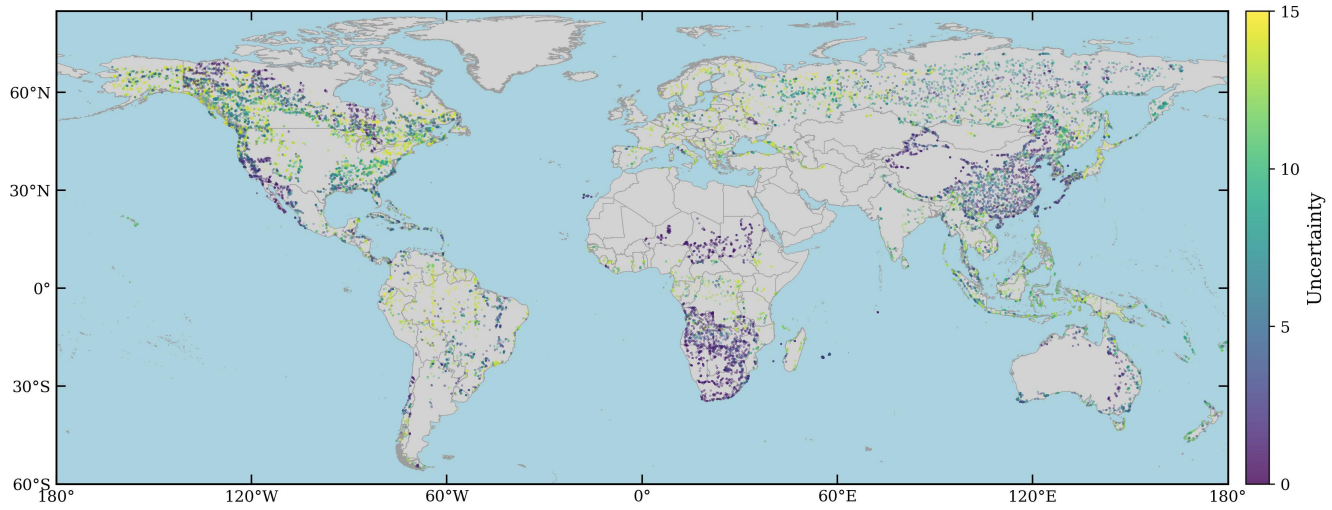

Figure 6: Global spatial distribution of the model-derived SUI for forest age estimation.

9. There are logical issues in breakpoint detection and forest age estimation. The paper's core assumption is that the starting point (t_start) of the last time segment detected by CCDC is the starting point of current forest age, a hypothesis with multiple problems. First, it confuses disturbance and recovery processes; misjudging a recovery breakpoint as a disturbance breakpoint will lead to systematic underestimation of forest age. Second, the lag in the starting point of stable segments is also an issue; even if a disturbance is correctly detected, t_start represents the starting several years of age underestimation. Finally, for old-growth forests over 40 years old that were already stable before 1985, CCDC may not detect any breakpoints, and the paper does not clearly explain how to estimate the age of these forests.

We acknowledge that relying solely on the raw t_{Start} of the final CCDC segment can indeed lead to a systematic underestimation of forest age due to the "spectral stabilization lag"—the temporal gap between biological establishment and the point where a statistical model can be stably initialized. To address this limitation, we have replaced the original simplistic assumption with an adaptive segment-fusion logic in Section 2.4.1. This updated framework explicitly distinguishes between the "rapid regrowth phase" and the "steady-state phase" of forest succession by applying differentiated recovery slope thresholds (>0.03 for natural forests and >0.04 for planted forests) within the multi-decadal trajectory. The algorithm now dynamically identifies if a stable terminal segment was preceded by a significant re-greening trajectory; if so, these successive segments are seamlessly fused, and the forest establishment year is back-propagated to the true onset of the initial recovery phase, effectively eliminating the multi-year lag and preventing the confusion between disturbance and stabilization breakpoints.

Regarding the reviewer's concern about old-growth forests, we have clarified in Section 2.3 and Section 4.3 that pixels remaining entirely stable without any detectable spectral breakpoints throughout the 1985-2024 observation window are assigned to an open-ended age class (≥ 40 years). This categorical approach prevents the false assignment of speculative empirical ages to mature stands that exceed the historical depth of the Landsat temporal archive, while successfully ensuring their correct representation as a lower-bound constraint in the global product. Furthermore, to address the potential uncertainties inherent in this process, we have introduced a pixel-wise uncertainty map (Fig. 6) in the revised manuscript. This map dynamically calculates the weighted average RMSE across fused segments, providing a spatially explicit metric of confidence that accounts for spectral variance throughout the entire identified successional sequence. We believe these methodological advancements, which move from post-hoc statistics to a priori ecological logic, comprehensively resolve the logical concerns raised.

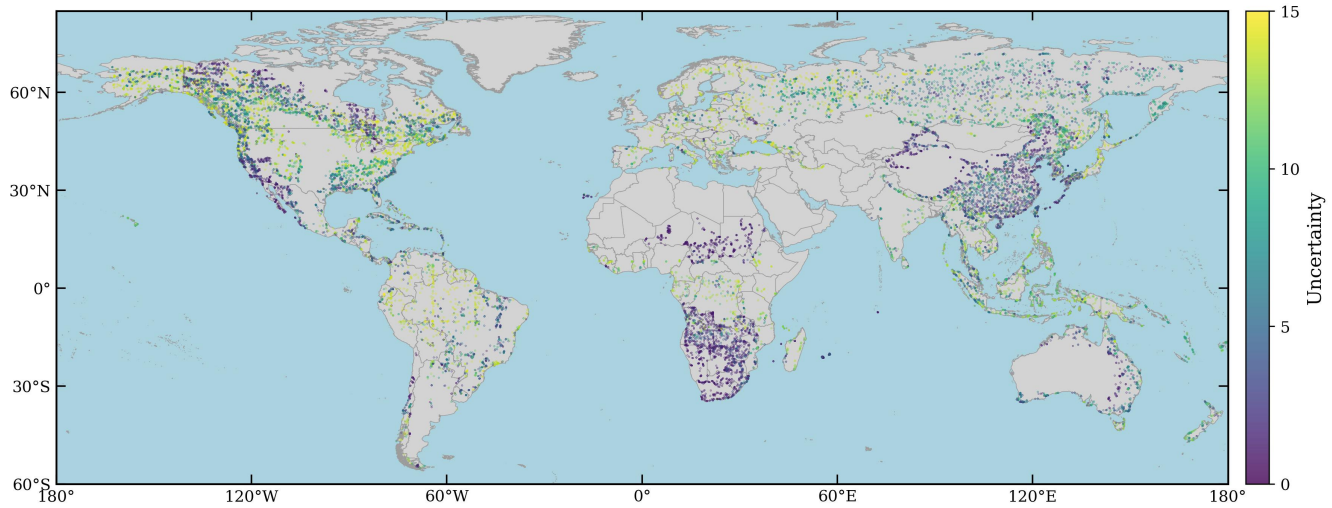

Figure 6: Global spatial distribution of the model-derived SUI for forest age estimation.

10. The claim of innovation in distinguishing natural and planted forests is unfounded. The paper claims that its innovation lies in being the "first global forest age product that distinguishes between natural and planted forests," but in reality, it does not adopt different processing methods for the two forest types. Both use CCDC detection results, and the "distinction" is only made in the final stage by displaying results and statistical accuracy separately based on the GNPF mask. This "distinction" is a posteriori and superficial rather than methodologically innovative. Natural and planted forests differ fundamentally in disturbance frequency, spectral characteristics, and age structure, warranting differentiated algorithm strategies to improve the accuracy of forest age estimation.

We agree with the reviewer that a simple post-hoc classification would be insufficient to capture the fundamental differences in the successional dynamics of natural and planted forests. Accordingly, we have fundamentally upgraded our methodological framework in Section 2.4.1 to implement a category-specific adaptive segment-fusion logic.

Rather than applying a uniform, undifferentiated processing chain, our revised methodology utilizes the GNPF mask as an a priori spatial constraint during the core algorithmic execution phase to geographically segregate NF and PF. The baseline fusion thresholds enforced within these two segregated domains were directly derived from the statistical distributions of our historical reference data, rather than being conceptualized as rigid constants. Specifically, we developed a dual-threshold fusion mechanism to reconcile the systematic spectral lag following disturbances (as detailed in Section 2.4.1). Recognizing that managed plantations typically undergo accelerated canopy closure and sharper spectral recovery trajectories compared to the more stochastic recovery of natural stands, the statistical analysis of our reference samples dictated a more stringent regrowth threshold (slope > 0.04) for PF, while a more lenient threshold (slope > 0.03) was assigned to NF. This differentiated approach ensures that the rapid successional phase is appropriately fused with the subsequent steady-state phase based on forest-specific recovery rates, allowing the forest establishment year to be accurately back-propagated to the true biological onset of the stand.

To provide a rigorous justification for these specific parameter selections and evaluate their global scalability, we have added a dedicated analysis and comprehensive discussion in Section 4.1 (Methodological standardization and parameter sensitivity). In this section, we explicitly elaborate on the environmental trade-offs and physical mechanisms governing our dual-threshold strategy across diverse biomes. We discuss how the more stringent 0.04

threshold for plantations effectively isolates the rapid biomass accumulation and intense canopy closure typical of intensive commercial species (e.g., *Eucalyptus* or *Pinus*), preventing high model stability during early successional stages from prematurely triggering a breakpoint reset and underestimating stand age. Conversely, we explain how the 0.03 threshold for natural forests accommodates the slow, stochastic secondary succession processes that are often heavily confounded by complex multi-layered canopy interactions and localized understory regeneration that blur overstory spectral signals (Tian et al., 2015). Furthermore, we address the strategic choice of maintaining a globally uniform dual-threshold benchmark rather than biome-specific adaptive functions, demonstrating that this standardized configuration is vital to preserve strict cross-continental comparability (Hansen et al., 2013) and avoid artificial spatial artifacts or disjunctions along eco-climatic boundaries. Our framework embeds these differentiated ecological constraints directly into the trajectory segmentation logic and thoroughly contextualizes their performance within the Discussion section.

11. There are credibility issues with the results. Figure 4b shows significant dispersion between predicted and observed values, particularly in high-age intervals (>25 years), where predicted values are significantly lower, consistent with the inherent limitations of the CCDC algorithm (inability to detect disturbances before 1985). However, the paper does not adequately discuss this systematic bias and its impact on the results, reducing the credibility and explanatory power of the results. Additionally, the uncertainty analysis of the forest age product is completely lacking.

We fully acknowledge that the "temporal ceiling" imposed by the multi-decadal Landsat archive (starting in 1985) is an inherent and fundamental constraint of optical time-series change detection, as canopy-clearing disturbances occurring prior to this timeline cannot be spectral-tracked. This boundary inevitably leads to a structural underestimation of absolute biological age for stands exceeding 25-30 years, as the core algorithm essentially captures the duration elapsed since the most recent major spectral reset rather than long-term absolute ontogeny.

To comprehensively resolve the concern regarding the lack of uncertainty analysis, we have substantially expanded our framework by implementing a dual-layer uncertainty appraisal encapsulating both verification-plot metrics and global pixel-level evaluations. First, we introduced Figure 11 to provide a robust, plot-level quantitative assessment of uncertainty by explicitly partitioning and displaying the probability density, medians, and interquartile ranges of predicted forest ages across different independent observed age groups. This visualization transparently demonstrates that while prediction precision remains exceptionally high for young forest cohorts (1-15 years), the structural dispersion and tail underestimation naturally expand as stands mature beyond the 25 year threshold. Second, we have generated a continuous, spatially explicit global confidence layer termed the Spatial Uncertainty Index (SUI), illustrated as Figure 6, which is derived by linearly scaling the model residuals from the CCDC time-series inversion to inform users of localized performance. Furthermore, we have comprehensively expanded the Discussion in Section 4.3 (Systematic biases, conceptual lags, and dataset limitations) to explicitly evaluate the underlying physical mechanisms driving this age-truncation bias, its environmental modulations (such as selective harvesting noise or rapid canopy closure saturation), and its subsequent implications for downstream carbon cycle modeling.

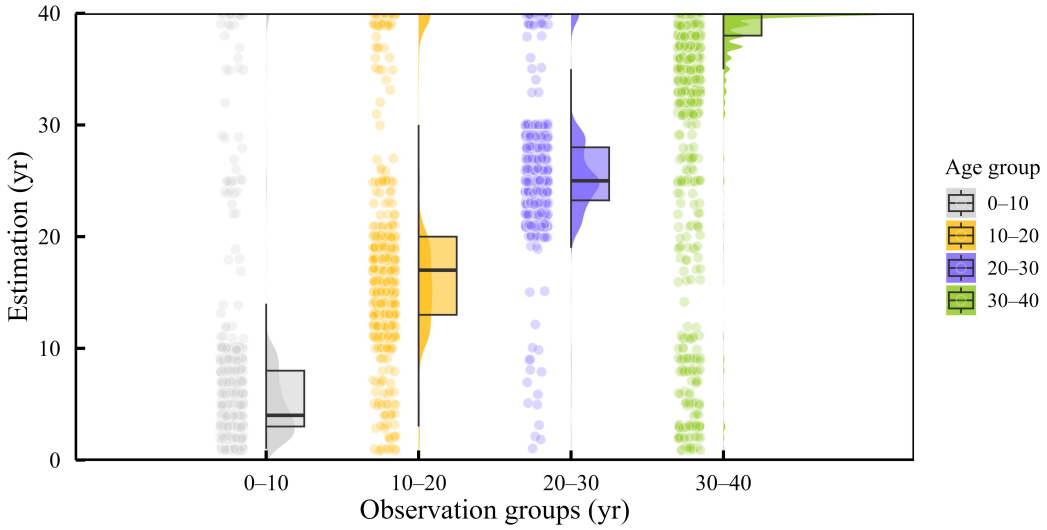

Figure 11: Distribution of estimated forest age for different observed age groups.

12. The paper exhibits non-compliance with writing standards and inadequate adaptation of submission templates. The paper's writing is relatively rough, with multiple non-standard aspects. Formatting issues include non-compliance with the ESSD submission template requirements for author affiliations, paragraph indentation, line spacing, and figure caption formatting. Repetition issues include duplicate content in "Acknowledgements" and "Financial support" (pages 21-22). Chart quality issues include insufficient resolution and unclear legend explanations for some charts. Language expression issues include multiple grammatical errors and unidiomatic expressions, suggesting the need for professional language polishing. The overall impression is that of a student's initial draft submitted without careful review by a supervisor. It is recommended that the author team conduct internal quality control to improve the overall quality of the paper.

We sincerely apologize for the formatting inconsistencies and language deficiencies in our original submission. We fully accept your criticism regarding internal quality control.

First, we have strictly re-aligned the manuscript with the official ESSD template, standardizing the author affiliations, paragraph indentations, and line spacing. Figure captions have been rewritten to be fully descriptive and self-contained, and the duplicate text between the "Acknowledgements" and "Financial support" sections has been completely eliminated.

Second, all figures and maps have been regenerated and exported at a high-resolution, publication-ready standard (300-600 DPI), with all legends, axes, and annotations clarified using precise biophysical units. Finally, the entire text has undergone professional language editing to eliminate grammatical errors and unidiomatic phrasing.

RC2: 'Comment on essd-2025-674', Anonymous Referee #2, 05 Mar 2026 reply

1. **Methodological Clarity for Age Assignment:**

The core methodology—assigning age based on the "latest stable segment" from CCDC—is logical for post-disturbance regrowth or afforestation. However, the manuscript would benefit from a more explicit discussion of how the algorithm handles the age estimation for mature natural forests that have not experienced a detected disturbance within the Landsat era (1985-2024). If no breakpoint is detected, does the algorithm default to assigning an age of "40+" (i.e., the full timespan of the study)? The current description in Section 2.4.2 and Figure 2 implies a breakpoint is always present. A clarification on how "stable,

old-growth" segments are treated is crucial for user interpretation of the dataset, especially given the high proportions of old-growth forests reported in Europe and the Americas.

We thank the reviewer for this critical observation regarding the treatment of mature forests and stable stands. To address these concerns, we have substantially revised Section 2.3 and Figure 2 to clarify our algorithmic logic. For pixels where no spectral breakpoint was detected throughout the 1985-2024 monitoring period, the entire timespan is treated as a single stable segment, which serves as our foundational baseline for identifying old-growth forests. Consequently, any pixel exhibiting a stable spectral trajectory throughout the observation window is systematically assigned to an open-ended minimum age class of ≥ 40 years, preventing stable stands in Europe and the Americas from being misclassified as young growth. Furthermore, we have refined the core definition of our product as the duration elapsed since the most recent detectable stand-replacing disturbance. This refined conceptual framework, coupled with the explicit "40+" assignment for undisturbed pixels in Figure 2 and Section 2.3, ensures the dataset remains scientifically robust while transparently communicating the inherent temporal constraints of the historical satellite archive.

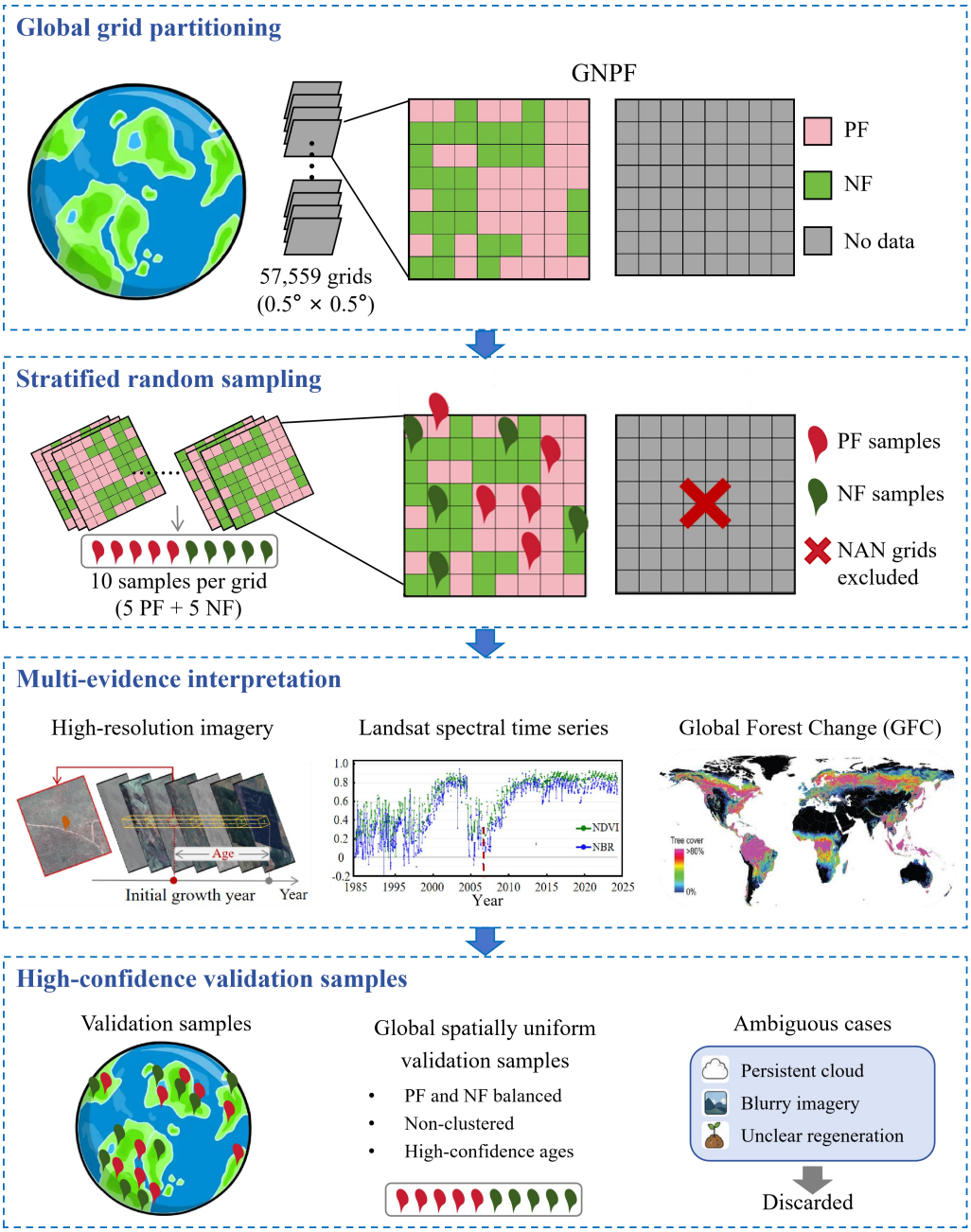

Figure 2: Workflow for generating validation samples using global grid-based stratified sampling.

2. **Sensitivity of NBR in Deciduous Forests**

The study relies heavily on the Normalized Burn Ratio (NBR) as the primary vegetation index for detecting disturbance and recovery events (Section 2.3). While NBR is indeed sensitive to structural and moisture changes, its performance can be seasonally variable, particularly in deciduous forests. In these ecosystems, the natural annual senescence and leaf-off periods can produce spectral signals that may be misinterpreted as disturbance events, or conversely, may obscure subtle disturbance signals. Additionally, the rapid green-up in spring could complicate the precise identification of a stand's establishment year. The manuscript would be strengthened by acknowledging this potential limitation and discussing how the CCDC algorithm's harmonic model (which accounts for seasonality) mitigates this risk, or if any additional post-processing was applied to filter out false positives caused by phenological cycles in temperate and boreal deciduous stands.

We appreciate the reviewer's professional insight regarding the phenological challenges in deciduous forests. We have addressed this by integrating both theoretical justifications and empirical evidence from our sensitivity analysis into the revised manuscript. Specifically, we clarify in Section 4.2 that while the NBR is sensitive to vegetative seasonality, the CCDC algorithm's harmonic regression framework effectively isolates predictable intra-annual variations—modeled via sine and cosine components—to distinguish cyclic phenological trends from true stand-replacing disturbances. Crucially, our systematic sensitivity analysis in Section 3.2 and Figure 8 provides support for this parameterization strategy: we demonstrated that enforcing a strict chiSquareProbability threshold of 0.99 is essential across all biomes, particularly in temperate and boreal zones, as it effectively suppresses spurious breakpoints triggered by seasonal leaf-off or senescent spectral noise. We also candidly acknowledge the inherent limitations of this approach, noting that extreme non-disturbance climatic anomalies or rapid spectral saturation during spring green-up remain persistent sources of boundary uncertainty. By combining robust harmonic modeling, strict statistical constraints validated through empirical sensitivity testing, and a transparent appraisal of these remaining errors, the revised manuscript now provides a more rigorous and reliable framework for global forest age estimation.

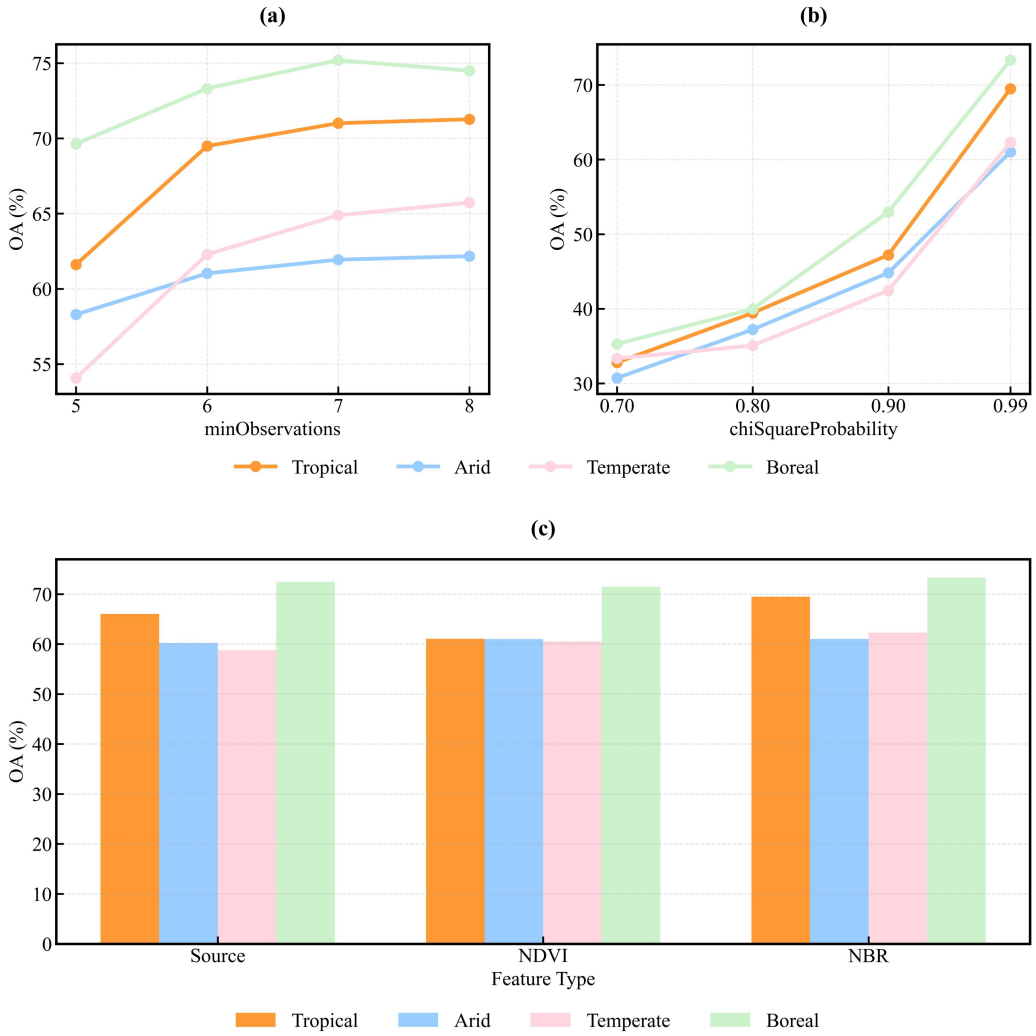

Figure 8: Sensitivity analysis of key temporal segmentation parameters and feature configurations across different climate zones. (a) OA sensitivity to minObservations; (b) OA sensitivity to chiSquareProbability under different climate zones; and (c) comparison of OA across feature configurations (Source, NDVI, and NBR) in different climate zones.

3. **Distinguishing Age from Ecological Succession:**

The current methodology defines forest age as the time since the last major disturbance (breakpoint). However, in many natural forest ecosystems, particularly in boreal and temperate zones, tree establishment is not instantaneous following a disturbance. Ecological succession often involves a lag phase where grasses and shrubs colonize an area before trees become established. Consequently, the "stand age" (time since disturbance) may significantly overestimate the "tree age" (actual age of the dominant cohort). The manuscript should explicitly acknowledge this distinction and discuss its potential implications for carbon modeling, as carbon accumulation rates in early-successional non-forest vegetation differ substantially from those in young tree stands.

We agree that in many ecosystems, particularly in boreal and temperate regions, the prolonged period of grass and shrub colonization following a major disturbance can lead to a temporal discrepancy between the physical

disturbance event and actual tree establishment. In the revised Section 4.3, we have explicitly acknowledged this conceptual nuance, clarifying that our CCDC-derived estimates strictly represent "stand age" (the time since the last detectable stand-replacing disturbance) rather than the absolute biological "tree age." We have also expanded our discussion on its subsequent implications for downstream carbon modeling, noting that carbon sequestration and biomass accumulation rates during early-successional canopy-open stages differ substantially from those in established, closed young forest stands.

To minimize the potential overestimation of tree age and isolate true forest recovery, our framework utilizes a highly stringent chiSquareProbability threshold of 0.99. As demonstrated in our sensitivity analysis (Section 3.2 and Figure 8b), this strict statistical constraint is vital to suppress spurious, transient breakpoints triggered by ephemeral early-successional vegetation or seasonal phenological noise, ensuring that the identified establishment year reflects a sustained, robust trajectory of long-term forest regeneration. Nevertheless, we openly admit that this biological delay in tree recruitment remains an inherent source of uncertainty in satellite-based chronosequences. By robustly characterizing our product as a "spectral proxy" and providing a transparent, scientifically honest discussion of these successional lags, the revised manuscript now offers a more rigorous and reliable foundation for regional ecological assessments.

4. **Partial Disturbance and Survivor Trees:**

A core assumption of the breakpoint-based method is that a detected disturbance clears the forest stand, resetting the age to zero. This assumption is often violated in reality. Many disturbances, such as low-severity fires, selective logging, or insect outbreaks, do not result in complete mortality. Surviving trees (remnants) can be decades or centuries older than the post-disturbance cohort. In such cases, assigning the entire pixel an age based on the last disturbance will systematically underestimate the true biological age of the forest and its existing carbon stock. The authors should address this limitation, perhaps by discussing how the prevalence of such partial disturbances varies by region and forest type, and how this might contribute to the higher RMSE or bias observed in certain areas (e.g., natural forests with complex age structures).

We sincerely appreciate the reviewer's insightful comments regarding the challenges of partial disturbances and survivor trees, which are critical for ensuring the scientific rigor of this study. We fully acknowledge the inherent limitation of breakpoint-based methods in capturing the absolute biological age of forests, particularly in cases of low-severity fires or selective logging where older remnant trees persist. To address this, we have refined both our methodology and product definitions in the revised manuscript. First, we have clarified in Section 2.3 that our product estimates "Young forest age," specifically defined as the duration elapsed since the most recent detectable stand-scale spectral reset. This conceptual distinction ensures academic transparency by separating spectral successional sequences from the total ontogenetic biological age of multi-aged stands. Methodologically, as detailed in Section 2.4.1, we implemented a category-specific adaptive segment-fusion logic that applies a more sensitive regrowth threshold (slope >0.03) for natural forests compared to plantations. This allows the model to better capture the subtle re-greening signals characteristic of post-partial disturbance natural succession, back-propagating the establishment year to the true onset of recovery. Concurrently, Section 2.3 clarifies that pixels remaining completely stable throughout the 1985-2024 observation window without any detectable spectral breaks are assigned to a minimum age class of ≥ 40 years, preventing undisturbed primary forests from being misclassified as young stands. To provide a spatially explicit assessment of reliability, we have incorporated a pixel-wise Spatial Uncertainty Index (SUI) map (Figure 6) derived directly from the model-inversion RMSE. As suggested by the reviewer, higher uncertainty clusters in structurally complex natural forests—such as those in the Amazon or boreal

regions—effectively serve as a diagnostic proxy for sub-pixel heterogeneity and partial disturbances, providing users with a necessary indicator of potential estimation bias in regions with complex canopy structures. These revisions, coupled with an expanded discussion in Section 4.3, ensure that the subsequent limitations regarding carbon stock estimation in partially disturbed forests are transparently and rigorously addressed.

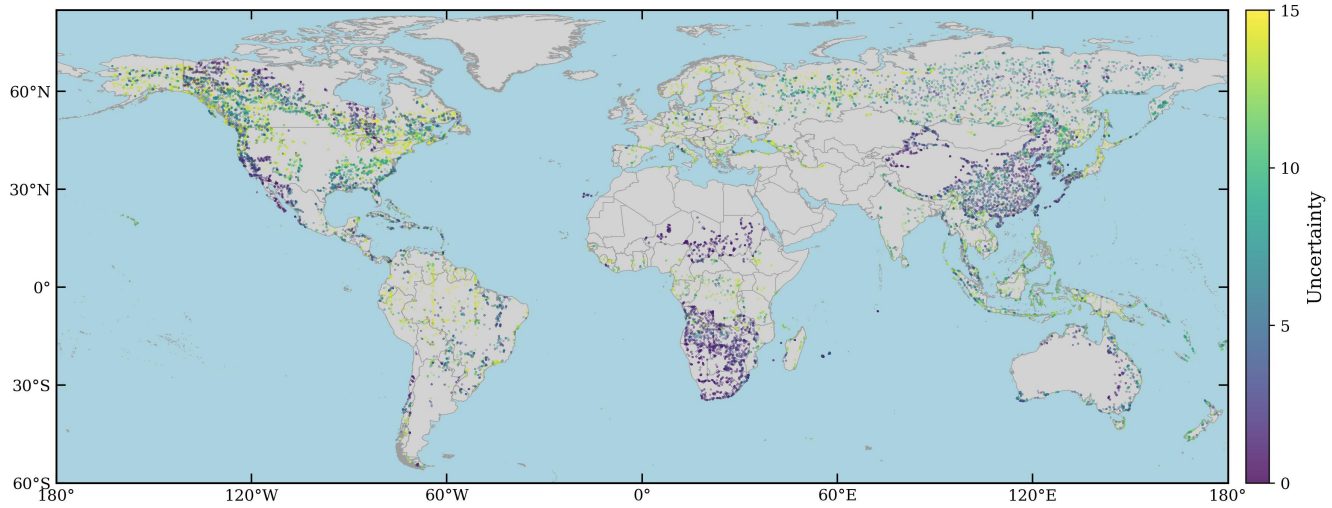

Figure 6: Global spatial distribution of the model-derived SUI for forest age estimation.